



# Nanoelectromechanical System Fourier Transform Infrared Spectroscopy (NEMS-FT-IR)

An introduction to the photothermal spectroscopy technique behind EMILIE™.  
Application Note M191

## Introduction

NEMS-FT-IR is a unique and powerful photothermal spectroscopy method that combines nanoelectromechanical systems (NEMS) with Fourier transform infrared (FT-IR) spectroscopy. This highly sensitive method is wavelength independent, making it ideal for studying a broad spectrum of samples. NEMS-FT-IR can be used to achieve limits of detection (LoD) down to the picogram level<sup>[1]</sup>, while built-in temperature control enables in-situ thermal desorption and stability studies<sup>[2]</sup>, paving the way to breakthroughs in materials characterization.

In NEMS-FT-IR, light from the FT-IR spectrometer is focused onto a highly temperature-sensitive NEMS resonator, called the EMILIE™ sampling and sensing chip, or EMILIE™ chip (Figure 1). The target analyte is deposited directly on the EMILIE™ chip (Figure 2) for sensing. When the analyte absorbs infrared light, the resulting heating-induced thermal expansion causes a reduction in the tensile stress of the EMILIE™ chip, leading to a change in its resonance frequency. EMILIE™'s frequency actuating and tracking electronics, PHILL, track these frequency changes in real time and report the data to the FT-IR's OPUS software, which generates the FT-IR absorption spectrum of the sample. NEMS-FT-IR produces spectra comparable to those obtained by transmission-FT-IR, allowing for interpretation using existing spectral libraries.

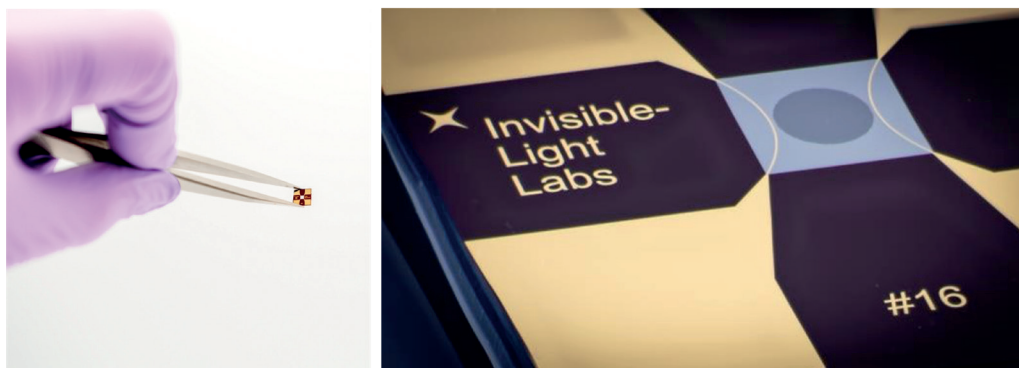


**Fig. 1**  
The EMILIE™ nanoelectromechanical sampling and sensing chip, also known as the EMILIE™ chip, is a NEMS resonator composed of a 50 nm -thick silicon nitride thin film.

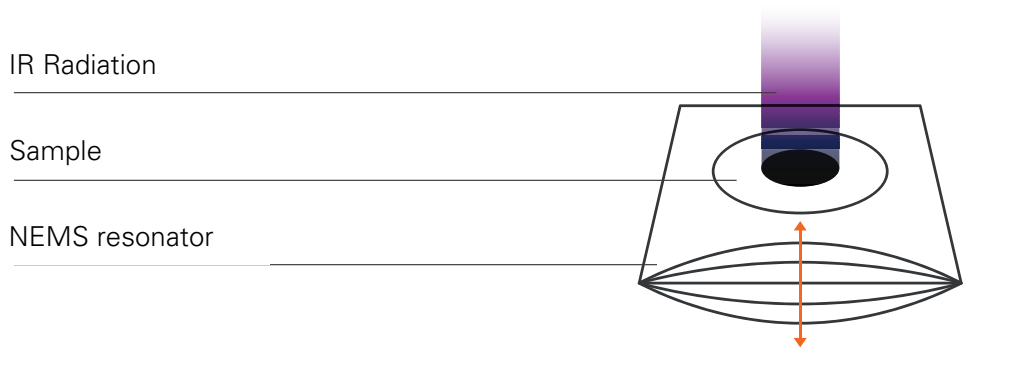


**Fig. 2**  
Estimated sampling times for different airborne particle sizes at a flow rate of 1 L/min.

## Spectral Range

NEMS-FT-IR distinguishes itself from other FT-IR techniques in that the sample is deposited directly onto the surface of the NEMS resonator, as schematically shown in Figure 2. This approach was first introduced in 2013 for the analysis of polymer nanoparticles in the visible (Vis)<sup>[3]</sup> and IR<sup>[4]</sup> spectral range. Since only the analyte itself absorbs and transduces the incident IR light, the nanomechanical photothermal sensing principle is inherently wavelength-agnostic, enabling spectroscopy across the UV<sup>[5]</sup> to IR regions of the electromagnetic spectrum<sup>[1,2,4,6,7]</sup>. It supports both dispersive spectroscopy, e.g., with a tunable quantum cascade laser (QCL)<sup>[1,4,6,7]</sup>, and FT-IR spectroscopy<sup>[1]</sup>. Bruker's VERTEX and INVENIO series FT-IR spectrometers (Figure 3 a) are able to span a wide spectral range from the near-IR to the far-IR and are compatible with EMILIE™. An example spectrum recorded with EMILIE™ on a VERTEX 80, spanning 6000 cm<sup>-1</sup> to 30 cm<sup>-1</sup> (1.67 μm to 333 μm), is shown in Figure 3 b.

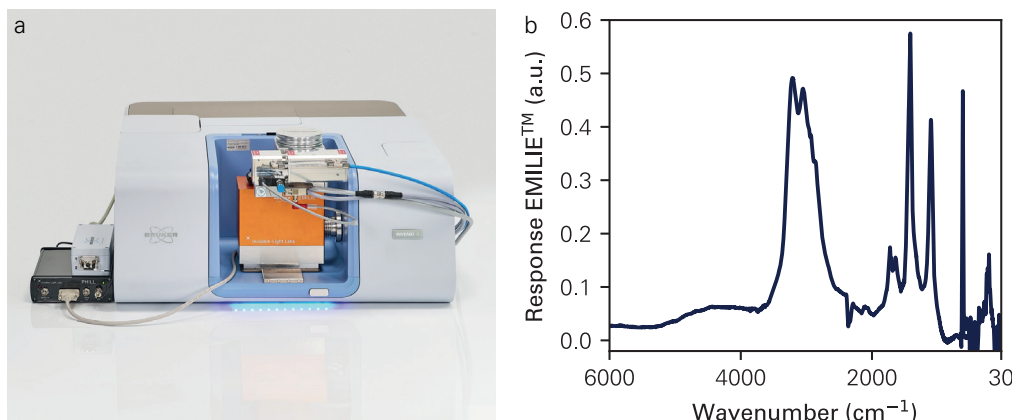


**Fig. 3**  
a) Photograph of EMILIE™ in the sample compartment of an INVENIO R.  
b) FT-IR spectrum of rural aerosol (particle size <700 nm, 15 min sampling time) recorded with EMILIE™ on a VERTEX 80, spanning 6000 cm<sup>-1</sup> to 30 cm<sup>-1</sup> (1.67 μm to 333 μm).

## Scattering and Reflectance

Light scattering and reflection can significantly impact absorption spectroscopy in both reflection and transmission mode, particularly when measuring particulate samples. In transmission spectroscopy, the detector captures less light due to scattering and reflection, creating artifacts in the absorption spectrum. In contrast, EMILIE™ is a photothermal method unaffected by these issues, as it measures absorption directly through photothermal heating. This avoids problems associated with reflections<sup>[8]</sup>, Mie scattering<sup>[9-11]</sup>, and Rayleigh scattering<sup>[12,13]</sup>, which are common in IR and UV-Vis spectroscopy, making NEMS-FT-IR a more reliable technique for accurate spectroscopic analysis of particulate samples.

## Sample Collection on the EMILIE™ Chip

The EMILIE™ chip is made from silicon nitride, which is a mechanically tough, chemically inert, and temperature-stable material. The EMILIE™ chip's central perforation enables efficient drop casting (Figure 4, a-b) and direct collection of airborne nanoparticles (Figure 4, c-d) as small as 10 nm with high efficiency<sup>[7, 14]</sup>. Other compatible deposition methods include spin coating, liquid

dipping, evaporation, molecular beam deposition, focused electron beam-induced deposition, and physical transfer (e.g., of 2D materials)<sup>[15]</sup>.

**Fig. 4**

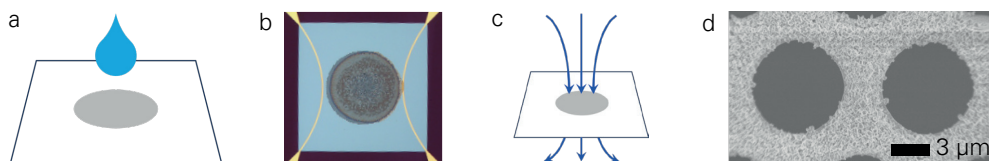
Some strategies to deposit a sample on the EMILIE™ chip.

a) Direct drop casting on the EMILIE™ chip.

b) Micrograph of an EMILIE™ chip featuring a sample drop casted with the help of the Drop Casting Accessory.

c) Schematic drawing of sample collection through aerosol impaction on the EMILIE™ chip.

d) Scanning Electron Microscopy image of a section of the perforated central area of the EMILIE™ chip on which nanoparticles have been collected via aerosol impaction.



## Temperature Control

Measurements with EMILIE™ are performed at a pressure of  $p < 1 \times 10^{-3}$  mbar. To prevent desorption of semi-volatile analytes during measurement, EMILIE™ allows cooling of the EMILIE™ chip during analysis. Conversely, the integrated temperature control also allows heating of the EMILIE™ chip. EMILIE™, therefore, allows for in-situ separation of individual compounds from complex mixtures<sup>[2]</sup>, or for thermal stability studies, for example.

## Sensitivity

While photon detectors can achieve single-photon sensitivity, thermal detectors like bolometers or pyroelectric detectors are typically constrained by electronic noise, including Johnson noise<sup>[16]</sup>. However, thermomechanical detectors operate on different principles, as they do not rely on electric detection to measure irradiated power. This fundamental difference means that EMILIE™ is not limited by electronic noise, which results in enhanced sensitivity<sup>[17]</sup>. The photothermal sensitivity of a nanomechanical resonator is given by its noise-equivalent power (NEP) with units  $[W/Hz^{1/2}]$  defined as

Equation 1

$$NEP = \frac{\sqrt{S_y(\omega)}}{R_p(\omega)}$$

with the fractional frequency noise power spectral density or frequency stability  $S_y(\omega)$  in units of  $[Hz^{-1}]$  and the responsivity to absorbed power  $R_p(\omega)$  with units of  $[W^{-1}]$ <sup>[18]</sup>.

## Responsivity

The power responsivity of a nanomechanical resonator with an eigenfrequency  $\omega_0$  is defined as<sup>[18]</sup>

Equation 2

$$R_p = \frac{\partial \omega_0}{\partial P} \frac{1}{\omega_0} H_{th}(\omega) = \frac{R_T}{G} H_{th}(\omega),$$

where  $R_T$  is the frequency responsivity to a change in temperature  $T$  and  $G$  is the thermal conductance.  $H_{th}(\omega)$  is a low-pass transfer function

Equation 3

$$H_{th}(\omega) = \frac{1}{\sqrt{1 + \omega^2 \tau_{th}^2}}$$

which drops off for signal frequencies faster than the resonator's thermal time constant  $\tau_{th} = C_{th}/G$ , with the resonator's heat capacity  $C_{th}$ .

Equation 2 shows, that the nanomechanical resonator essentially acts as a thermometer with a temperature responsivity  $R_T$  of the resonator, defined as<sup>[18]</sup>

Equation 4

$$R_T = \frac{\partial \omega_0}{\partial T} \frac{1}{\omega_0}$$

The physical effect underlying  $R_T$  is two-fold: 1) temperature-induced softening of the Young's modulus  $E$ , and 2) thermal expansion affecting the tensile stress  $\sigma$ .

In stress-free structures such as beams and plates, the dominant photothermal effect is temperature-induced softening with  $R_T \approx \alpha_E/2$ , where  $\alpha_E$  is the thermal softening coefficient. Conversely, in prestressed structures like strings and the EMILIE™ chip, frequency detuning occurs due to changes in tensile stress through thermal expansion. Here, the temperature responsivity is  $R_T \approx \alpha_{th}E/(2\sigma)$ , with  $\alpha_{th}$  representing the thermal expansion coefficient of the resonator material.<sup>[18]</sup>

The temperature responsivity of resonators under tensile stress, such as the EMILIE™ chip, is enhanced by a factor of  $(E/\sigma \gg 1)$ , which is generally much greater than one for most materials. This comparison underscores the superiority of pre-stressed strings and drumhead resonators for temperature sensing over beam and plate resonators. **The EMILIE™ chip exhibits a temperature response enhancement factor exceeding 1000.**

The responsivity (Equation 2) further scales inversely with the thermal conductance  $G = G_{cond} + G_{rad}$ , where the operation in vacuum eliminates contributions due to convection. Here,  $G_{cond}$  and  $G_{rad}$  are the conductances due to conductive and radiative heat transfer, respectively. It has been shown that for the 50 nm thin silicon nitride drumhead resonators, such as the EMILIE™ chip, radiative heat transfer starts to become significant for sizes larger than 1 mm.<sup>[19, 20]</sup>

The responsivity of a square drumhead resonator that is heated evenly can be derived and is given by<sup>[18, 21]</sup>

Equation 5

$$\begin{aligned} R_p &= R_T G^{-1} H_{th}(\omega) \\ &= \frac{\alpha_{th} E}{2\sigma(1-\nu)} [2\pi^2 \kappa h + 8\epsilon L^2 \sigma_B T^3]^{-1} H_{th}(\omega) \end{aligned}$$

with the resonator's Poisson's ratio  $\nu$ , the thermal conductivity  $\kappa$ , thickness  $h$ , emissivity  $\epsilon$ , and lateral size  $L$ .  $\sigma_B$  is the Stefan–Boltzmann constant.

## Frequency stability and noise contributors

The very high sensitivity of EMILIE™ is due in part to its excellent frequency stability. The frequency stability  $S_y(\omega)$  in Equation 6 is the sum of the four following noise contributions

Equation 6

$$S_y(\omega) = S_{y,th}(\omega) + S_{y,d}(\omega) + S_{y,T}(\omega) + S_{y,ph}(\omega)$$

which are thermomechanical noise  $S_{y,th}(\omega)$ , detection noise  $S_{y,d}(\omega)$ , temperature fluctuation noise  $S_{y,T}(\omega)$ , and photothermal back-action noise  $S_{y,ph}(\omega)$ <sup>[18, 21]</sup>. While there are other noise contributions, such as adsorption-desorption noise, these are the dominating noise sources in nanomechanical resonators such as EMILIE™.

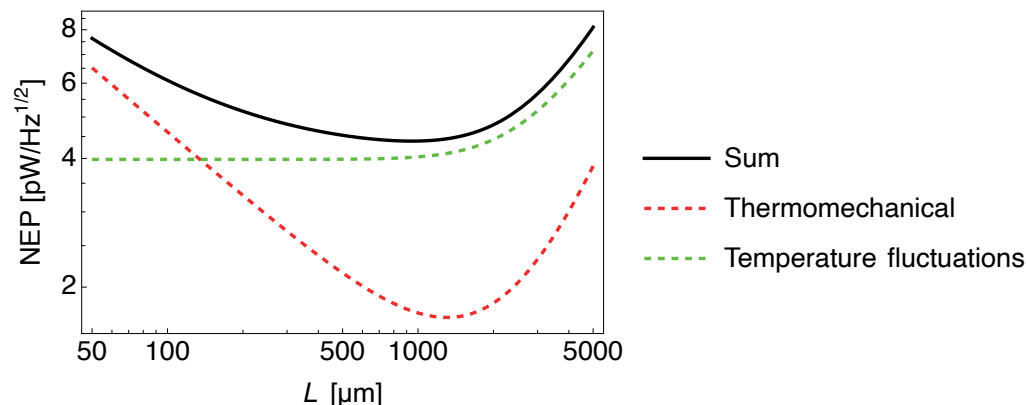
Thermomechanical noise and temperature fluctuation noise are the two fundamental sources that ultimately limit the sensitivity of nanomechanical photothermal spectroscopy. Ideally, detection noise should be lower than thermomechanical noise to provide optimal performance. EMILIE™ uses a low-noise electrodynamic detection scheme.

Photothermal back-action noise typically can be neglected in low-noise light sources such as Globars used in FT-IR spectrometers. However, it can become a significant noise source in light sources with a high relative intensity noise, such as QCLs<sup>[22]</sup>.

The NEP (Equation 1) can be estimated based on the thermomechanical and temperature fluctuation noise contributions alone. The NEP for a silicon nitride drumhead resonator, such as the EMILIE™ chip, and when operated in a closed-loop scheme, such as a self-sustaining oscillator (SSO) as used in EMILIE™<sup>[23, 24]</sup>, is shown in Figure 5.

**Fig. 5**

Noise equivalent power model prediction (Equation 1) for a square 50 nm thin bare silicon nitride drumhead with a tensile stress of 50 MPa at room temperature, such as the EMILIE™ chip.



### Limit of detection of EMILIE™

The limit of detection (LoD) can be estimated from the NEP and the photothermal heating induced by a sample for a given probing light power. The number of molecules  $n$  that give a signal equivalent to the noise can be calculated from  $n = NEP / (IA)$ , with the probing light irradiance  $I$  in units of  $[W/m^2]$  and the absorption cross-section of a single molecule  $A$  in unit of  $[m^2]$ .

For the estimated  $NEP \approx 4 \text{ pW/Hz}^{1/2}$ , as shown in Figure 5, the LoD can be estimated for a low noise thermal light source with a power of 100 nW and a focal beam diameter of 1 mm<sup>2</sup>. For a protein sample, e.g., BSA with a molecular mass of 66.5 kDa and an absorption cross-section of  $7.3 \times 10^{-20} \text{ m}^2$  at a wavelength of 6 μm<sup>[25]</sup>, this results in an estimated LoD (3 sigma) of 180 pg for an integration time of 1 second. This is a good approximation for the LoD of EMILIE™ used in conjunction with an FT-IR and in agreement with experimental results<sup>[1]</sup>.

### Key advantages of EMILIE™

- Broad Spectral Range – Wavelength-independent sensing enables measurements across the entire infrared range.
- High Sensitivity at Room Temperature – No need for cryogenic cooling to achieve picogram-level detection limits.
- Direct Sample Collection – Analytes can be deposited directly onto the EMILIE™ chip from airborne aerosols, powders, or liquid dispersions.
- Resilience to Optical Artifacts – Performance is unaffected by light scattering or reflectance, ensuring robust signal interpretation of particulate samples.
- Integrated Temperature Control – Allows in-situ thermal desorption and temperature stability studies.
- Low Intrinsic Noise – Nanomechanical design ensures a high signal-to-noise ratio.
- Low Detection Limit – Capable of detecting minute sample quantities, down to the picogram scale.

## References

- <sup>[1]</sup> Popovic, J.T., Hiesberger, J., Šesto, Luhmann, N., E., Giesriegl, A., Lafleur, J.P., and Schmid, S., Nanoplastic Analysis with Nanoelectromechanical System Fourier Transform Infrared Spectroscopy, arXiv:2504.10192 (2025).
- <sup>[2]</sup> Luhmann, N., West, R. G., Lafleur, J. P. & Schmid, S. Nanoelectromechanical infrared spectroscopy with in situ separation by thermal desorption: NEMS-IR-TD. *ACS Sensors* 8, 1462–1470 (2023).
- <sup>[3]</sup> Larsen, T., Schmid, S., Villanueva, L. G. & Boisen, A. Photothermal Analysis of Individual Nanoparticulate Samples Using Micromechanical Resonators. *ACS Nano* 7, 6188–6193 (2013).
- <sup>[4]</sup> Yamada, S., Schmid, S., Larsen, T., Hansen, O. & Boisen, A. Photothermal infrared spectroscopy of airborne samples with mechanical string resonators. *Analytical Chemistry* 85, 10531–10535 (2013).
- <sup>[5]</sup> Kirchhof, J. N. et al. Nanomechanical absorption spectroscopy of 2D materials with femtowatt sensitivity. 0–7 (2023).
- <sup>[6]</sup> Andersen, A. J. et al. Nanomechanical IR spectroscopy for fast analysis of liquid-dispersed engineered nanomaterials. *Sensors and Actuators, B: Chemical* 233, 667–673 (2016).
- <sup>[7]</sup> Kurek, M. et al. Nanomechanical Infrared Spectroscopy with Vibrating Filters for Pharmaceutical Analysis. *Angewandte Chemie* 129, 3959–3963 (2017).
- <sup>[8]</sup> Bassan, P. et al. Reflection contributions to the dispersion artefact in FT-IR spectra of single biological cells. *Analyst* 134, 1171–1175 (2009).
- <sup>[9]</sup> Bassan, P. et al. Resonant Mie scattering in infrared spectroscopy of biological materials—understanding the ‘dispersion artefact’. *Analyst* 134, 1586–1593 (2009).
- <sup>[10]</sup> Bassan, P. et al. Resonant Mie scattering (RMieS) correction of infrared spectra from highly scattering biological samples. *Analyst* 135, 268–277 (2010).
- <sup>[11]</sup> Dazzi, A., Deniset-Besseau, A. & Lasch, P. Minimising contributions from scattering in infrared spectra by means of an integrating sphere. *Analyst* 138, 4191–4201 (2013).
- <sup>[12]</sup> Porterfield, J. Z. & Zlotnick, A. A simple and general method for determining the protein and nucleic acid content of viruses by UV absorbance. *Virology* 407, 281–288 (2010).
- <sup>[13]</sup> Rüdert, M., Vormittag, P., Hillebrandt, N. & Hubbuch, J. Process monitoring of virus-like particle reassembly by diafiltration with UV/vis spectroscopy and light scattering. *Biotechnology and bioengineering* 116, 1366–1379 (2019).
- <sup>[14]</sup> Schmid, S., Kurek, M., Adolphsen, J. Q. & Boisen, A. Real-time single airborne nanoparticle detection with nanomechanical resonant filter-fiber. *Scientific Reports* 3, 3–7 (2013).
- <sup>[15]</sup> West, R. G., Kanellopoulos, K. & Schmid, S. Photothermal microscopy and spectroscopy with nanomechanical resonators. *The Journal of Physical Chemistry C* 127, 21915–21929 (2023).
- <sup>[16]</sup> Rogalski, A. *Infrared and Terahertz Detectors*, Third Edition. (CRC Press, 2019). doi:10.1201/b21951.
- <sup>[17]</sup> Cary, H. H. Infrared radiation detector employing tensioned foil to receive radiation. (1969).
- <sup>[18]</sup> Schmid, S., Villanueva, L. G. & Roukes, M. L. *Fundamentals of nanomechanical resonators*, 2nd edition. (Springer International Publishing AG Switzerland, 2023).
- <sup>[19]</sup> Piller, M. et al. Thermal radiation dominated heat transfer in nanomechanical silicon nitride drum resonators. *Applied Physics Letters* 117, 034101 (2020).
- <sup>[20]</sup> Zhang, C., Giroux, M., Nour, T. A. & St-Gelais, R. Radiative heat transfer in freestanding silicon nitride membranes. *Physical Review Applied* 14, 024072 (2020).
- <sup>[21]</sup> Kanellopoulos, K. et al. Comparative analysis of nanomechanical resonators: Sensitivity, response time, and practical considerations in photothermal sensing. *Microsystems & Nanoengineering* 11, 28 (2025).
- <sup>[22]</sup> Akhgar, C. K. et al. The next generation of IR spectroscopy: EC-QCL-based mid-IR transmission spectroscopy of proteins with balanced detection. *Analytical Chemistry* 92, 9901–9907 (2020).
- <sup>[23]</sup> Bešić, H., Demir, A., Steurer, J., Luhmann, N. & Schmid, S. Schemes for tracking resonance frequency for micro- and nanomechanical resonators. *Physical Review Applied* 20, 024023 (2023).
- <sup>[24]</sup> Bešić, H., Demir, A., Vukićević, V., Steurer, J. & Schmid, S. Adaptable frequency counter with phase filtering for resonance frequency monitoring in nanomechanical sensing. *IEEE Sensors Journal* (2024).
- <sup>[25]</sup> Schwaighofer, A., Akhgar, C. K. & Lendl, B. Broadband laser-based mid-IR spectroscopy for analysis of proteins and monitoring of enzyme activity. *Spectrochimica Acta Part A: Molecular and Biomolecular Spectroscopy* 253, 119563 (2021).

